

PRAF2 stimulates cell proliferation and migration and predicts poor prognosis in neuroblastoma

LISETTE P. YCO^{1,2,4}, DIRK GEERTS^{5,6}, JAN KOSTER⁵ and ANDRÉ S. BACHMANN¹⁻⁴

¹Department of Pharmaceutical Sciences, College of Pharmacy, University of Hawaii at Hilo, Hilo, HI 96720;

²University of Hawaii Cancer Center and ³Department of Cell and Molecular Biology, John A. Burns School of Medicine, University of Hawaii at Manoa, Honolulu, HI 96813; ⁴Department of Molecular Biosciences and Bioengineering, University of Hawaii at Manoa, Honolulu, HI 96822, USA; ⁵Department of Human Genetics, Academic Medical Center, University of Amsterdam, 1105 AZ Amsterdam; ⁶Department of Pediatric Oncology/Hematology, Sophia Children's Hospital, Erasmus University Medical Center, 3015 GE Rotterdam, The Netherlands

Received July 19, 2012; Accepted September 7, 2012

DOI: 10.3892/ijo.2013.1836

Abstract. Prenylated Rab acceptor 1 domain family, member 2 (PRAF2) is a novel 19-kDa protein with four transmembrane-spanning domains that belongs to the PRAF protein family. Neuroblastoma (NB) is the most common malignant extracranial solid tumor of childhood that originates in primitive cells of the developing sympathetic nervous system. We investigated the correlation of PRAF2 mRNA expression to NB clinical and genetic parameters using Affymetrix expression analysis of a series of 88 NB tumors and examined the functional role of PRAF2 in an NB cell line using RNA interference. We found that high PRAF2 expression is significantly correlated to several unfavorable NB characteristics: *MYCN* amplification, high age at diagnosis, poor outcome and high INSS stage. The shRNA-mediated PRAF2 downregulation in the SK-N-SH NB cell line resulted in decreased cellular proliferation, migration and matrix-attachment. These findings were confirmed in NB patient tumor samples, where high PRAF2 expression is significantly correlated to bone and bone marrow metastasis, the main cause of death in NB patients. The present study shows that PRAF2 plays an essential role in NB tumorigenesis and metastasis.

Introduction

Neuroblastoma (NB) is the most common and deadly extracranial solid tumor of childhood. NBs, together with the more differentiated, less aggressive ganglioneuromas and ganglioneu-

roblastomas, form the neuroblastic tumors. They are all derived from migratory, primitive precursor cells of the developing sympathetic nervous system. NB tumors are graded according to INSS stage, where stages 1 and 2 represent low-risk tumors and stages 3-4 high-risk tumors (1,2). Children that are diagnosed with NB when they are over 1 year of age generally suffer from the advanced stages of the disease. These NB tumors, especially stage 4, can rapidly spread to regional lymph nodes and then to distal bone and bone marrow, resulting in very poor patient prognosis. Infants diagnosed with NB can present a unique pattern of metastatic spread (stage 4S, S = Special) to the liver and skin, but only rarely to bone or bone marrow. Remarkably, these metastasized tumors usually undergo spontaneous regression and patients have excellent prognosis (1,2). Important prognostic features of NB tumors are therefore INSS stage and patient age at diagnosis. In addition, recurrent genomic aberrations like *MYCN* gene amplification can be used for patient stratification (1,2). Unfortunately, these combined NB features are still too limited to ensure early proper treatment stratification and new prognostic markers are needed. In addition, NB treatment, especially of metastasized tumors is still not sufficiently efficient and more insight is needed into the molecular pathways involved in NB metastasis.

Prenylated Rab acceptor 1 domain family, member 2 (PRAF2, initially described as JM4) is a 19-kDa protein with four transmembrane-spanning domains. PRAF2 belongs to the PRAF family of vesicle transport-associated proteins. Members of the PRAF family are structurally related and contain a large prenylated Rab acceptor 1 (PRA1) domain. These PRAF proteins are localized in the ER, Golgi and vesicular structures of the cell (3,4). PRAF2 was first discovered as an interacting protein of human chemokine receptor 5 (CCR5) (3) and of human glycerophosphoinositol phosphodiesterase (GDE1/MIR16) (5). Human PRAF2 is highly expressed in numerous tissues: small intestine, lung, spleen, pancreas and most significantly in the brain. Furthermore, overexpression of PRAF2 is observed in tumor tissue samples of breast, colon, lung and ovary, compared to matched normal tissue samples (4,6,7).

The other two members of PRAF protein family (PRAF1 and PRAF3) have already been extensively studied and their

Correspondence to: Dr André S. Bachmann, Department of Pharmaceutical Sciences, College of Pharmacy, University of Hawaii at Hilo, 34 Rainbow Drive, Hilo, HI 96720, USA
E-mail: andre@hawaii.edu

Key words: cell proliferation, metastasis, neuroblastoma, patient survival, pediatric cancer, prenylated Rab acceptor 1 domain family, member 2

biological function has been characterized. In fact, many of these studies associated PRAF1 and PRAF3 with several well-known cancer signaling pathways. For instance, PRAF1 (also known as Rabac1, PRA1, prenylin and Yip3), a Golgi complex, post-Golgi vesicle and endosomal transmembrane protein, was initially identified to interact with small GTPase proteins that regulate intracellular vesicle trafficking (8-10). In addition, PRAF1 has a crucial role in colorectal tumorigenesis by regulating the nuclear transport of β -catenin in TCF/ β -catenin signaling (11). PRAF1 functions in Epstein-Barr virus (EBV)-induced transformation: it binds and modulates the anti-apoptotic activity of BHRF1, an EBV-encoded early protein and enhances nuclear import of the oncogenic EBV-encoded latent membrane protein 1 (LMP1) (12,13).

PRAF3 (also known as JWA, GTRAP3-18 and Arl6-IP5) is an integral ER membrane protein that is upregulated by retinoic acid (RA) and then activates the excitation amino acid carrier 1 (EAAC1), a primary neuronal glutamate transporter (14,15). PRAF3 is also defined as a potential inhibitor of cancer cell migration by regulation of the MAPK signaling pathway and F-actin cytoskeleton (16). PRAF3 was found to inhibit melanoma metastasis by suppressing integrin $\alpha v \beta 3$ signaling, a key factor in tumor metastasis. Downregulation of PRAF3 in melanoma cells significantly increased integrin $\alpha v \beta 3$ expression (both at mRNA and protein level) and accelerated cell adhesion, migration and invasion *in vitro* and enhanced melanoma lung metastasis *in vivo*.

Unlike PRAF1 and PRAF3, PRAF2 has not yet been widely studied and its functional role therefore remains largely unknown. Previously, our lab found PRAF2 as a candidate prognostic marker of neuroblastic tumors. We observed high level of PRAF2 mRNA in most neuroblastic tumor samples. We also found that PRAF2 protein is strongly expressed in all 24 NB cell lines tested, including SK-N-SH (17). Despite these discoveries, the molecular role of PRAF2 in NB tumorigenesis, or in other tumors in which it is highly expressed, has remained unexplored. Therefore, in this study, we generated NB cell lines that stably downregulate endogenous PRAF2 expression by RNA interference (RNAi). We used these PRAF2 knock-down NB cell lines to investigate the function of PRAF2 in NB tumorigenesis. Metastasis is the main cause of death in NB patients, but its underlying mechanisms remain elusive. Considering the role of its homolog PRAF3 in melanoma invasion and metastasis, we were especially interested to find out if PRAF2 is involved in NB metastasis and therefore focused on cell migration and matrix-attachment.

Materials and methods

Cell line culture. The human NB cell line SK-N-SH was purchased from the American Type Culture Collection (Manassas, VA). Cells were maintained in RPMI-1640 (Mediatech Inc., Manassas, VA) containing 10% heat-inactivated fetal bovine serum (FBS) (Invitrogen Corp., Carlsbad, CA) at 37°C in a humidified atmosphere containing 5% CO₂. Cells were counted using a hemocytometer in the presence of trypan blue (Sigma-Aldrich, St. Louis, MO).

Construction of stable PRAF2 knockdown NB cell lines. HuSH 29-mer short hairpin RNA (shRNA) expression constructs

against PRAF2 (shPRAF2) and GFP (scrambled; as a negative control) were purchased from Origene Technologies (Rockville, MD). SK-N-SH cells were seeded in 6-well culture plates (Greiner Bio-One Inc., Monroe, NC) at a concentration of 5.0×10^5 cells per well and transfected with 4 μ g shPRAF2 or scrambled plasmid using Lipofectamine 2000 (Invitrogen). Transfected cells were incubated for 24 h at 37°C as described above and subsequently selected using 1.0 μ g/ml puromycin (Sigma-Aldrich). After selection for 2 weeks, cells retaining the shPRAF2 (SK-shPRAF2) or scrambled expression vector (SK-Sc) were maintained at 100 ng/ml puromycin.

Western blot analysis. For total protein isolation, medium was removed by aspiration, adherent cells were washed twice in ice-cold DPBS (Dulbecco's phosphate buffered saline, Mediatech) and cell lysates prepared by scraping on ice into radioimmunoprecipitation assay (RIPA) buffer [20 mM Tris-HCl (pH 7.5), 0.1% (w/v) sodium lauryl sulfate, 0.5% (w/v) sodium deoxycholate, 135 mM NaCl, 1% (v/v) Triton X-100, 10% (v/v) glycerol, 2 mM EDTA], supplemented with Complete Protease Inhibitor Cocktail (Roche Diagnostic Corp., Indianapolis, IN) and phosphatase inhibitors (20 mM sodium fluoride and 0.27 mM sodium vanadate). Lysate samples were resuspended by rotation at 50 rpm and 4°C for at least 30 min and clarified by centrifugation for 15 min at 14,000 rpm and 4°C. The supernatant was stored at -20°C until further use. Total protein concentration was determined by Bradford dye reagent protein assay (Bio-Rad Laboratories Inc., Richmond, CA). Laemmli buffer (Bio-Rad) containing 10% (v/v) β -mercaptoethanol (VWR International, Brisbane, CA) solution was added to the lysates and boiled for 5 min. Ten micrograms total protein was resolved by 12% sodium dodecyl sulfate-polyacrylamide gel electrophoresis (SDS-PAGE) and electrotransferred onto a polyvinylidene difluoride (PVDF) membrane (Immobilon-P, VWR International). Membranes were incubated with rabbit polyclonal PRAF2, peptide-blocked rabbit polyclonal PRAF2 (PRAF2-P) (QED Bioscience, San Diego, CA), or rabbit monoclonal α -tubulin (Cell Signaling Technology, Danvers, MA) primary antibodies. The membranes were then washed and incubated with enhanced chemiluminescence (ECL) rabbit or mouse IgG, horseradish peroxidase (HRP)-linked secondary antibody (GE Healthcare Biosciences, Pittsburgh, PA). Subsequently, membranes were again washed and protein-antibody complexes were detected using ECL plus western blotting detection reagents (GE Healthcare Biosciences) and Blue Lite Autorad Film (ISC BioExpress, Kaysville, UT). Bands were quantified using the Bio-Rad Multi Imager and its Quantity One Quantification software.

Cell viability assay. Cells (1.0×10^4 cells in 0.1 ml) were seeded in 96-well microtiter plates (Greiner Bio-One Inc.) and incubated for 24, 48 or 72 h. For each time point, 20 μ l of CellTiter 96 Aqueous One Solution Reagent (Promega Bioscience Inc., San Luis Obispo, CA) was added to wells and incubated at 37°C for 3 h. The conversion of MTS tetrazolium to soluble formazan in cell cultures was measured at 490 nm using an HTS 7000 Plus Microplate Reader (Perkin-Elmer, Waltham, MA). Optical density (OD) readings, proportional to the number of viable cells, were calculated and evaluated using Microsoft Excel.

Cell proliferation assay. Cell proliferation was determined with the EMD BrdU Cell Proliferation Assay kit (EMD Biosciences Inc., San Diego, CA), following the manufacturer's protocol. Briefly, cells were seeded and grown as above. For each time point, 20 μ l of BrdU label was added to cell cultures and allowed to incorporate into DNA for 2 h at 37°C. Cells were fixed and denatured, upon addition of 200 μ l fixative/denaturing solution, for 30 min at room temperature. Anti-BrdU antibody (1:100) was added and incubated for 1 h at room temperature to bind incorporated BrdU label. Unbound BrdU antibodies were removed by washing three times with wash buffer. Peroxidase goat anti-mouse IgG HRP conjugate (200 μ l) was added and incubated for 30 min at room temperature. Cells were washed twice with wash buffer and once with deionized water. Cells were incubated in 100 μ l substrate solution for 15 min in the dark at room temperature, after which 100 μ l stop solution was added to the cells. Absorbance was measured immediately at 450 nm using the HTS 7000 Plus Microplate Reader. OD readings, representing cell proliferation, were calculated and evaluated using Microsoft Excel.

Cell cycle analysis. Cells (1.0×10^6 cells in 1 ml) were seeded in 60-mm culture plates (Greiner Bio-One Inc.) and incubated for 24 h. Cells were trypsinized, washed twice in DPBS and counted using a hemocytometer. Cells were pelleted by centrifugation at 1,500 rpm and resuspended to 2.0×10^6 cells/ml DPBS. One million cells per 5 ml polystyrene tube (Fisher Scientific, Pittsburgh, PA) were fixed by slow addition of 1.5 ml 70% ice-cold ethanol (Fisher Scientific) under gentle vortexing. Ethanol-fixed cells were incubated in an ice bath for 1 h, pelleted again and washed twice in DPBS. Cells were then resuspended and stained with 0.5 ml PI/RNase staining buffer (Becton-Dickinson Biosciences, San Jose, CA) for 15 min at room temp in the dark. Finally, stained cells were resuspended in 1 ml DPBS. A minimum of 10,000 cells was analyzed using the FACScan flow cytometry instrument and its CellQuest software (Becton-Dickinson).

Wound-healing assay. Cell migration *in vitro* was determined using the wound-healing assay as described by Valster *et al* (18). Briefly, cells were cultured to confluency in a 6-well culture plate and wounds scratched through the monolayer using a sterile 20 μ l pipette tip. Cells were carefully washed several times with DPBS to remove floating cells and fresh medium was added back without detaching cells. Cell images were taken at 0, 6, 12, 18 and 24 h using a Leica DM-IL digital microscope (Leica Microsystems, Buffalo Grove, IL). The rate of wound closure was calculated as the ratio of the migrated cell surface area divided by the total surface area.

Adhesion assay. Immulon-2 96-well microtiter plates (Fisher Scientific) were pre-coated with 10 μ g/ml fibronectin (FN), vitronectin (VN), or laminin (LM) (all from Sigma) or not coated and incubated overnight at 4°C. Substrates were removed by aspiration and blocking solution (2% BSA heat-inactivated in DPBS) was added to coated and uncoated wells and incubated for 2 h at room temperature. Afterwards, wells were washed with serum-free RPMI. Cells (50,000 cells in 0.1 ml) were seeded and incubated for 90 min at 37°C and then washed with DPBS until cells in the BSA-only coated control wells were completely

removed. Attached cells were fixed with 50% (v/v) glutaraldehyde in DPBS for 20 min at room temperature, after which the solution was removed by aspiration and the cells allowed to air-dry for 5 min. Cells were then stained with 0.5% crystal violet in 20% methanol for 45 min and washed three times with DPBS. The cells were air-dried and solubilized in 10% acetic acid for 30 min. Absorbance was measured at 560-590 nm using a Perkin-Elmer HTS 7000 Plus microplate reader. OD readings, representing the number of adherent cells, were calculated and evaluated using Microsoft Excel.

Affymetrix DNA micro-array hybridization and analysis. The Affymetrix NB tumor dataset Versteeg-88 contains the mRNA expression profiles of 88 NB tumors with documented genetic and clinical features and has been described (19). Total RNA was extracted from frozen NBs containing >95% tumor cells and Affymetrix HG-U133 Plus 2.0 micro-array analysis (Affymetrix, Santa Clara, CA, USA) performed as described (20). The Versteeg-88 set has been deposited for public access in a MIAME-compliant format through the Gene Expression Omnibus (GEO) database at the NCBI website (21) under number GSE16476. Public domain datasets Hiyama-51 (GSE16237), Jagannathan-100 (GSE19274), Łastowska-30 (GSE13136), Maris-101 (GSE3960) were also from the NCBI GEO site, the Oberthuer-251 set (E-TABM-38) was from EMBL-EBI ArrayExpress. Annotations and clinical data for the tissue samples analyzed are available from <http://www.ncbi.nlm.nih.gov/geo/query/> or <http://www.ebi.ac.uk/arrayexpress/> thru their GEO or EMBL-EBI ID's, respectively. CEL data for all data-sets were downloaded and analyzed as previously described (20). Briefly, gene transcript levels were determined from data image files using GeneChip operating software (MAS5.0 and GCOS1.0, from Affymetrix). Samples were scaled by setting the average intensity of the middle 96% of all probe-set signals to a fixed value of 100 for every sample in the dataset, allowing comparisons between micro-arrays. The TranscriptView genomic analysis and visualization tool was used to check if probe-sets had an anti-sense position in an exon of the gene (<http://bioinfo.amc.uva.nl/human-genetics/transcriptview/>). The Affymetrix probe-set selected for PRAF2, 203456_at meets these criteria and showed significant expression in all 88 samples in the Versteeg-88 set. Analyses were performed using R2; an Affymetrix analysis and visualization platform developed in the Department of Human Genetics at the Academic Medical Center, University of Amsterdam. R2 can be accessed at: <http://r2.amc.nl>.

Statistical analyses. PRAF2 correlation with survival probability was evaluated by Kaplan-Meier analysis using the Wilcoxon log-rank test as described (22). PRAF2 expression and correlation with NB clinical and genetic features were determined using the non-parametric Kruskal-Wallis test; correlation with other gene expressions was calculated with a 2log Pearson test. The significance of a correlation is determined by $t = R/\sqrt{(1-R^2)/(n-2)}$, where R is the correlation value and n is the number of samples. Distribution measure is approximately as t with n-2 degrees of freedom. The statistical significance of the effects on NB cell viability, proliferation, cell cycle and adhesion were determined using the statistical Student's t-test. For all tests, P<0.05 was considered statistically significant.

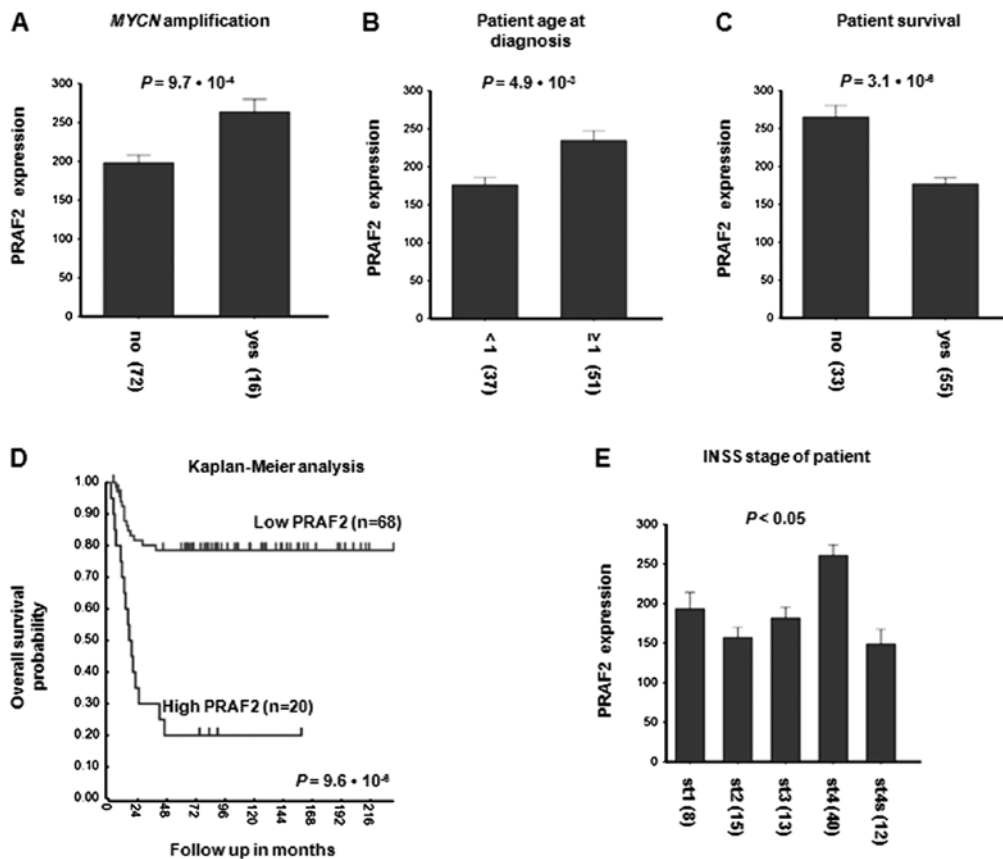


Figure 1. Correlation of PRAF2 expression with clinical features of NB. PRAF2 mRNA expression was examined by Affymetrix micro-array in the Versteeg-88 series of 88 NB tumors with full clinical description and compared with important clinical parameters. PRAF2 mRNA expression correlates with (A) tumor *MYCN* amplification, (B) age at diagnosis, (C) patient survival during follow-up, (D) patient survival probability and (E) INSS stage of the disease. (A) NB patients with tumor *MYCN* amplification (16 samples) expressed significantly higher PRAF2 levels than patients without tumor *MYCN* amplification (72 samples; $P=9.7 \times 10^{-4}$). (B) NB patients that were diagnosed above the age of 1 year (higher risk; 51 samples) expressed significantly higher PRAF2 tumor levels than patients that were diagnosed below this age (lower risk; 34 samples; $P=4.9 \times 10^{-3}$). (C) NB patients that were still alive at the time of analysis (55 samples) expressed significantly higher PRAF2 tumor levels than patients who had died before that time (33 samples; $P=3.1 \times 10^{-6}$). (D) PRAF2 gene expression correlates with NB patient survival prognosis. Shown is a Kaplan-Meier graph representing the survival prognosis of 88 NB patients based on high or low expression levels of PRAF2. The survival probability of NB patients (follow-up >216 months) with high PRAF2 expression is significantly lower than of patients with low PRAF2 expression. For the Kaplan-Meier analysis, the P-values were calculated for all 72 groups tested (minimum group size = 8). For PRAF2, the 20 'high' versus the 68 'low' group represents the highest P-value ($P=9.6 \times 10^{-6}$), but the P-value was <0.05 for all groups from 28 low/60 high to 77 low/11 high. Also when the 88 tumors were divided using the median or average PRAF2 expression, P-value was <0.05, showing that PRAF2 expression has a robust correlation with survival. Statistical analysis was performed with the Wilcoxon log-rank test. (E) Children with NB tumor stages 1, 2, 3 or 4S (8, 15, 13 or 12 samples, respectively) expressed significantly lower-level PRAF2 tumor levels than children with tumor stage 4 (40 samples; stage 4 comparison to any other stage has $P < 0.05$). Statistical analysis of (A-C) and (E) was performed using the non-parametric Kruskal-Wallis tests, but for reasons of representation, the bar plots show actual expression values. Numeric values in parentheses indicate the number of evaluated NB patient tumor samples. For expression value calculations in all panels, see Materials and methods.

Results

PRAF2 expression correlates with NB parameters indicative of poor outcome. We have previously shown that PRAF2 expression is higher in neuroblastic tumors than in most other cancers. To explore the potential role of PRAF2 in NB, the most aggressive neuroblastic tumor, we investigated PRAF2 expression in a new cohort of NB tumors. We analyzed a series of 88 NB tumors for which extensive genetic and clinical features were available from patient files ('Versteeg-88', Academic Medical Center at the University of Amsterdam) using the genome-wide HG-U133 Plus 2.0 Affymetrix DNA microarray. We found that PRAF2 was efficiently expressed in all 88 NB samples. Since *MYCN* amplification is the most dependable prognostic marker and is associated with very poor prognosis, we investigated a possible correlation PRAF2 expression. Fig. 1A shows that

PRAF2 is significantly higher in *MYCN*-amplified tumors than in tumors with a diploid *MYCN* gene complement ($P=9.7 \times 10^{-4}$; Fig. 1A). In addition, PRAF2 expression is higher in patients diagnosed when they are older than 1 year old than in younger patients ($P=4.9 \times 10^{-3}$; Fig. 1B). Since high PRAF2 expression is correlated to two unfavorable clinical parameters of NB, it was not surprising that PRAF2 expression in tumor samples taken from NB patients that have since died is significantly higher than that in NB from patients that are still alive at the time of analysis ($P=3.1 \times 10^{-6}$; Fig. 1C). To assess the predictive value of PRAF2 expression, we performed Kaplan-Meier analysis. The most significant P-value was found when the Versteeg-88 set was divided into a group of 20 with high and of 68 with low expression of PRAF2 mRNA, but also for most other groupings within the set, high PRAF2 expression was significantly indicative for poor outcome (Fig. 1D). Survival of patients with low

Table I. PRAF2 correlations with clinical parameters in additional NB tumor sets in the public domain.

Set	Kaplan-Meier	Survival	INSS	MYCNA	Platform
Hiyama-51	ND	Lower in alive	ST4 highest	NS	Affymetrix HG-U133 Plus 2.0
Jagannathan-100	ND	Lower in low-risk	ST3 higher than ST4	Higher in MNA	Illumina HWG 6V2
Łastowska-30	ND	ND	ST4 highest ^a	NS	Affymetrix HG-U133 Plus 2.0
Maris-101	ND	ND	ST4 highest	Higher in MNA	Affymetrix HG-U95 Av2
Oberthuer-251	Poor prognosis	Lower in alive	ST4 highest	Higher in MNA	Amexp255
Versteeg-88	Poor prognosis	Lower in alive	ST4 highest	Higher in MNA	Affymetrix HG-U133 Plus 2.0

Analysis of PRAF2 mRNA expression correlation with survival prognosis (by Kaplan-Meier analysis), survival, INSS and MYCN gene amplification as determined by Affymetrix or Illumina genome-wide mRNA expression array analysis. Analysis was performed in five public NB tumors sets: Hiyama-51 (GEO16237), Jagannathan-100 (GEO19274), Łastowska-30 (GEO13136), Maris-101 (GEO3960), Oberthuer-251 (EBI ArrayExpress set E-TABM-38) and the results obtained compared with the Versteeg-88 NB set (GEO16476) described in this report. Differences shown are significant ($P < 0.05$), unless indicated otherwise. NS, not significant. ND, data are not available for that data-set. ^aST4 has the highest expression; but the difference with ST3 is not significant. All sets contained samples with MYCN gene amplification (MNA) at at least average occurrence in patients. Despite the variety of sets and array analysis methods used, the correlations observed between PRAF2 expression and clinical parameters in the Versteeg-88 set compare well with those obtained for the additional five public NB tumors sets indicating that this is a very robust observation. For expression value calculations and statistical analyses see Materials and methods.

PRAF2 expression ($n=68$) was ~80% for up to 216 months, while that for patients with high PRAF2 expression ($n=20$) dropped to 20% within 48 months ($P=9.6 \times 10^{-6}$; Fig. 1D). Not surprisingly therefore, when PRAF2 expression was investigated with respect to INSS stage, we found that PRAF2 expression was highest in the most aggressive, stage 4 tumors, that often and rapidly metastasize to lymph nodes, bone and bone marrow and are the major cause of neuroblastoma-related death. Of note, PRAF2 expression was significantly higher in stage 4 tumors than in any other stage ($P < 0.05$; Fig. 1E), including stage 4S tumors. Since these tumors can metastasize to skin and liver but have an extremely good prognosis, this would suggest PRAF2 has a role in clinically important, but not 4S metastasis processes. Together, the results from the Versteeg-88 set strongly suggest a role for PRAF2 in tumor cell survival and aggressive tumor growth and metastasis. To investigate the robustness of these observations in the NB series presented in this report, we investigated the correlations found between PRAF2 expression and NB clinical parameters in five additional NB series in the public domain (Table I). We observed similar patterns for PRAF2 mRNA expression in these independent series, suggesting that the results obtained with the Versteeg-88 set are representative. However, as noted before, the molecular role of PRAF2 in these processes is still completely unknown.

Generation of stable PRAF2 knockdown NB cells using shRNA.

To confirm a role for PRAF2 in NB progression and to gain insight into the molecular pathways downstream of PRAF2 function, we generated PRAF2 knockdown NB cell lines using shRNA. We stably transfected PRAF2 shRNA (shPRAF2) or scrambled control shRNA (Sc) expression vectors into SK-N-SH NB cells, grew shRNA-expressing clones and analyzed the PRAF2 protein content of these clones by western blotting. We used the peptide-blocked PRAF2 antibody (PRAF2-P) to confirm that the PRAF2 bands we detected are specific. PRAF2-P antibody prevents PRAF2 from binding. As expected, PRAF2-P antibody did not recognize PRAF2 (Fig. 2A). PRAF2

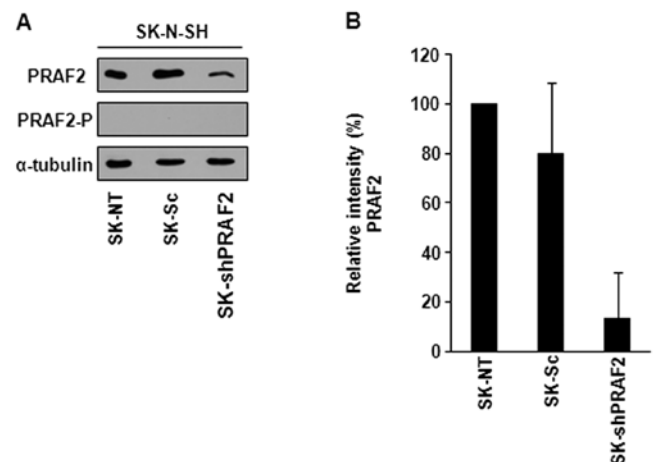


Figure 2. Downregulation of native PRAF2 in NB cells. (A) Whole cell lysates were prepared from SK-N-SH cells that were left untreated (-NT) or transfected with Sc shRNA (-Sc) as negative controls, or with PRAF2 shRNA (-shPRAF2). Total protein (10 μ g) was used to prepare western blots, which were probed with PRAF2, PRAF2-P and α -tubulin antibody. PRAF2-P antibody prevents PRAF2 from binding and was used as a control for the specificity of the PRAF2-reactive protein bands. (B) Quantification of bands using Bio-Rad Multi Imager and Quantity One Quantification software and normalized relative to the α -tubulin band. PRAF2 protein content of -shPRAF2 cells was 80% (SK-N-SH) lower than that of untreated, -NT cells. These data are representative of three individual experiments ($n=3$); bars, mean \pm SD.

shRNA-transduced SK-N-SH cells (SK-shPRAF2) showed ~80% decrease in PRAF2 protein expression in comparison with control cells.

Upon establishment of this PRAF2 knockdown NB cell line, we investigated the effect of PRAF2 downregulation in these NB cells by observing their phenotypic morphology and viability. To this end, we seeded equal numbers of shPRAF2- and Sc-expressing cells. Strikingly, we found that SK-shPRAF2 cells were less able to grow confluent than both SK control cells, non-transfected (-NT) and scrambled (-Sc) control cells, after

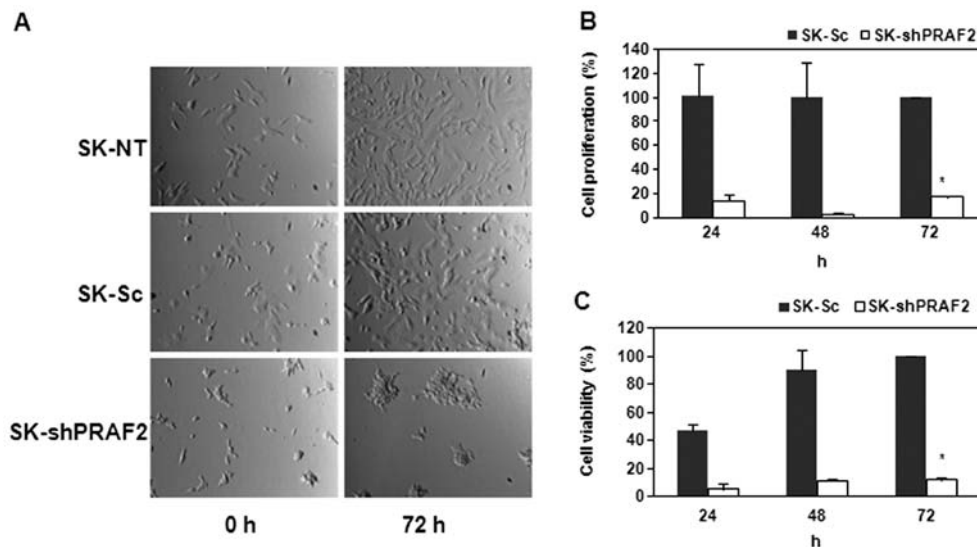


Figure 3. Effects of PRAF2 downregulation on NB cell morphology and proliferation. Equal amounts of SK-N-SH, SK-Sc and SK-shPRAF2 were seeded at low density and allowed to grow for 0, 24, 48 or 72 h. Photomicrographs of cells were recorded after 0 or 72 h at 10x magnification using a Leica DM-IL digital microscope. PRAF2-silenced NB cell line SK-shPRAF2 grew significantly slower than control cells (A). Indeed, the cell proliferation rate of SK-shPRAF2 cells was strongly reduced as determined using BrdU cell proliferation assay (B). Moreover, the cell viability of SK-shPRAF2 cells was reduced and confirmed the microscope-based observation as determined by MTS assay after 24-, 48- and 72-h incubation (C). The cell viability and proliferation results of the SK-shPRAF2 cells were normalized to SK-Sc at 72-h incubation. All assays were performed in duplicate and are presented as mean \pm SD from three independent experiments (n=6). *P<0.005 compared with control cells.

72-h incubation (Fig. 3A). These data suggest downregulation of PRAF2 inhibits cell growth and/or adhesion in NB cells.

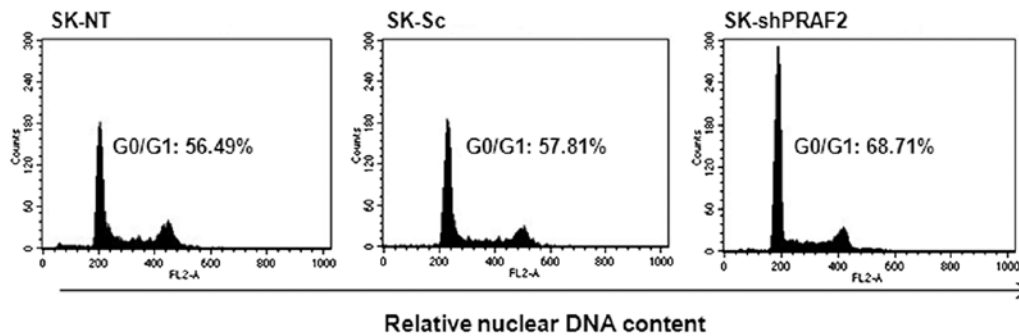
PRAF2 is essential for NB cell proliferation. We therefore examined whether PRAF2 knockdown regulates the proliferation of NB cells. First, we used the MTS assay to determine the cell viability of SK-shPRAF2 compared to that of SK control cells. As shown in Fig. 3C, SK-Sc showed steadily increasing metabolic activity indicative of viable cell growth, while SK-shPRAF2 remained at very low levels even after 72-h incubation. We further investigated the effect of PRAF2 downregulation in SK-N-SH cell proliferation using the BrdU cell proliferation assay. We found that downregulation of PRAF2 significantly suppressed the cell proliferation of SK-N-SH cells by ~80% compared to that of SK-Sc after 24, 48 or 72 h (Fig. 3B). The steady decrease in BrdU incorporation suggests that SK-shPRAF2 cells are severely defective in DNA synthesis and hardly undergo cell division. Together, these results show that silencing PRAF2 suppresses the proliferation of NB cells. Similar observations were made with another stable NB cell line (data not shown).

PRAF2 regulates G₁-S cell cycle transition in NB. Since PRAF2 downregulation effectively suppresses the proliferation rate of NB cells and also seems to inhibit DNA synthesis, we wanted to further analyze if this effect is linked with cell cycle abrogation. In order to examine this, we performed cell cycle analysis by PI staining and FACS analysis of SK-shPRAF2 nuclei 24 h after seeding and compared with those of SK control cells -NT and -Sc. As shown in Fig. 4, we observed an increase in G₁ population (~68%) in the SK-shPRAF2 cells compared with SK-NT (~55%) and SK-Sc (~58%) control cells. The increase in G₁ was accompanied by a similar decrease in S and G₂/M phase. No changes were apparent in the sub-G₁ frac-

tion, suggesting the observed decrease in proliferation was not due to an increase in apoptosis. Together, these data strongly indicate that PRAF2 downregulation inhibits the proliferation of NB cells by causing a G₁ cell cycle arrest, explaining at least part of the decreased cell growth observed in Fig. 3.

PRAF2 downregulation inhibits NB cell migration. The results obtained in Fig. 4 clearly suggest that PRAF2 expression was important for NB cell growth, but decreased confluence, observed in Fig. 3 could also result from lower cell adhesion efficiency. PRAF2 expression is highest in ST4 NB tumors (Fig. 1E), which often metastasize. We investigated PRAF2 expression in correlation with NB metastasis. Strikingly, PRAF2 expression was notably higher in both bone and bone marrow-metastasized tumors ($P=8.5 \times 10^{-5}$; Fig. 5) than in local tumors. These results show that high level of PRAF2 is also associated with NB metastasis.

By using the SK-shPRAF2 cells, we tested the effect of PRAF2 knockdown on NB cell migration *in vitro*. We used the wound-healing assay to investigate and compare the migration ability of SK-shPRAF2 cells with -NT and -Sc control cells. As shown in Fig. 6A and B, PRAF2 knockdown produced SK-N-SH cells with a marked delay in wound closure, >24 h, while both -NT and -Sc control cells showed complete wound closure after only 12-h incubation. Finally, we examined whether downregulation of PRAF2 regulates NB cell attachment on fibronectin, vitronectin and laminin using an adhesion assay. The results show that PRAF2 knockdown considerably decreased the cell attachment ability of SK-N-SH cells on all three substrates: fibronectin (~75%), vitronectin (~80%) and laminin (~55%) (Fig. 6C). These data confirm a role for PRAF2 in regulating NB tumor cell migration and suggest involvement of PRAF2 in high-stage NB, providing urgently needed clues for unraveling the mechanisms involved in NB metastasis.



	Cell cycle (% Total cells)		
	G0/G1	S	G2/M
SK-NT	56.49 ± 3.13	22.66 ± 4.58	18.01 ± 4.52
SK-Sc ¹	57.81 ± 0.35	21.75 ± 0.40	13.74 ± 4.42
SK-shPRAF2	68.71 ± 2.17	18.77 ± 4.16	11.12 ± 3.08

Figure 4. PRAF2 downregulation causes G₁ cell cycle arrest in SK-N-SH cells. Equal amounts of SK-N-SH cells (SK-shPRAF2, SK-NT and SK-Sc) were seeded at low density and allowed to grow for 24 h. Cells were then harvested by trypsinization and counted and 1.0x10⁶ cells were fixed in 70% ethanol and stained with PI for 15 min. Stained cells were then analyzed for their relative DNA content using FACS analysis using a Becton-Dickinson FACScan flow cytometer. Data represent the mean ± SD from three independent experiments (n=3) with P<0.005 compared to control cells. ¹SK-Sc data represent two independent experiments (n=2).

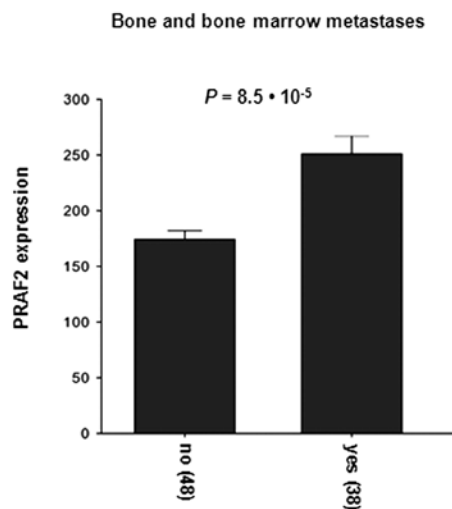


Figure 5. PRAF2 levels are increased in NB patients with metastatic disease. PRAF2 mRNA expression was compared with NB metastasis in the Versteeg-88 series. Bone and bone marrow metastases are significant predictors of poor outcome in NB. Children with NB metastasized to the bone or bone marrow (n=38) showed significantly higher PRAF2 expression than children without metastases (48 samples; P=8.5x10⁻⁵, data available for 86 of 88 tumors). For other details see Table I.

Discussion

Previously, our lab found that PRAF2 expression is higher in neuroblastic tumors than in all other cancers examined (17). To explore the role of PRAF2 in NB, the most aggressive neuroblastic tumor, we investigated PRAF2 expression in a new cohort of NB tumors. Here, we found that PRAF2 is significantly correlated with unfavorable genetic and clinical hallmarks of NB. PRAF2 tumor expression is notably higher

in NB patients with tumor *MYCN* amplification, in high-risk patients of >1 year-old or with high-stage disease and in patients who died during follow-up. We therefore hypothesized that PRAF2 plays an important role in tumorigenesis and progression of NB.

Cancer is regularly defined as a disease of the cell cycle: the uncontrollable proliferation of tumor cells is often due to the deregulation of cell cycle machinery (23,24) and NB tumors can have mutations in several cell cycle checkpoints, most notably the G₁-S transition (25). Since PRAF2 is overexpressed in NB tumor cells, we used RNAi to knock down the level of PRAF2 in NB cells and examine possible cellular viability effects. Strikingly, PRAF2 knockdown NB cells showed decreased cell growth in comparison with control NB cells. This is in apparent contrast with a recent study in which no growth retardation was detected when expression of PRAF2 was depleted (23). We also noted an increase of cell population at G₁ phase in PRAF2 knockdown NB cells. Therefore, these data suggest that high PRAF2 expression, in cooperation with the decreased G₁-S threshold caused by mutated checkpoint molecules, allows NB tumor cells to leave the G₁ phase and continue the cell cycle.

Previous studies showed that reduction of PRAF3, a PRAF2 homologue, enhances adhesion and invasion of melanoma cells *in vitro* and melanoma metastasis *in vivo* by regulating integrin $\alpha v \beta 3$ (26). We therefore evaluated if PRAF2 is also involved in NB metastasis. Cancer metastasis is a complex process, in which tumor cells need to detach from their primary site, migrate, adhere at a distal location and invade this new host environment (24, 27). Interestingly, Affymetrix analysis showed that overexpression of PRAF2 is strongly correlated with NB metastasis. In contrast to the role of PRAF3 in melanoma cell migration, we found that PRAF2 downregulation delays NB cell migration. PRAF3 expression is associated with

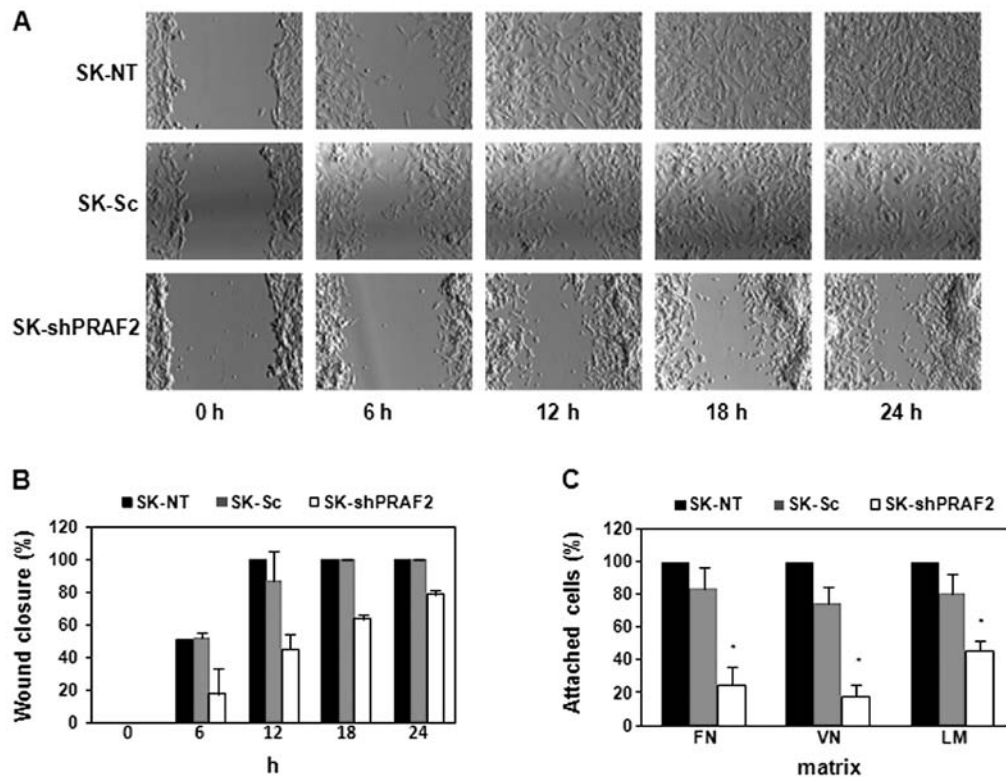


Figure 6. PRAF2 downregulation regulates NB cell migration and attachment. SK-N-SH cells (SK-shPRAF2, SK-NT and SK-Sc) were grown to full confluence in 6-well plates and subjected to monolayer wounding (A and B), or were seeded in fibronectin- (FN), vitronectin- (VN), or laminin (LM)-coated 96-well plates, allowed to grow for 3 h and subjected to an adhesion assay (C). After monolayer wounding, photomicrographs were taken at 0, 6, 12, 18 and 24 h. The wound healing in cells with silenced PRAF2 (SK-shPRAF2) was significantly slower than in SK-NT or SK-Sc control cells (A). The wound-healing assays were quantified by measurement of the percentage of the gap closed during the time indicated (B). While SK-shPRAF2 cells required >24 h, identically treated SK-NT and SK-Sc control cells closed the gap within 12 h. The cell attachment of cells was determined using an adhesion assay with three different matrices (FN, VN and LM) and coloring with crystal violet (C). SK-shPRAF2 cells showed significantly lower adhesion capability than the SK-NT or SK-Sc controls cells. Each assay was performed in duplicate and data are presented as mean \pm SD from three independent experiments (n=6). *P<0.005 compared with control cells.

good prognosis in NB (data not shown). Moreover, depletion of PRAF2 decreased cell-matrix attachment ability of NB cells in fibronectin, vitronectin and laminin, three of the major components of extracellular matrix.

PRAF family proteins act by virtue of their Rab-binding activity. Most probably therefore, PRAF2 is involved in the formation of exosome-like vesicles, which were recently discovered as a novel mechanism in tumor metastasis that depend on Rab function and cause changes in cell cycle, extracellular matrix, as well as migration/invasion (28,29). Indeed, we found that PRAF2 expression is correlated with these processes. In addition, the expression of several crucial exosome-associated Rab and extracellular matrix genes correlates with that of PRAF2 in NB (data not shown). Future studies will therefore investigate the role of PRAF2 in this mechanism in detail.

In conclusion, we found a clinical implication of PRAF2 expression in a cohort of 88 NB tumors. These observations were validated *in vitro* by silencing PRAF2 in NB cells which led to reduced proliferation, migration and cell-matrix adhesion. In contrast to PRAF3 which inhibits cell migration and induces apoptosis (16,30), our experiments suggest that the novel PRAF2 protein plays a prominent role in NB tumorigenesis and metastasis and thus may be of value as a novel target in NB.

Acknowledgements

We gratefully acknowledge Drs Dana-Lynn Koomoa, Tamas Borsics, Joe Ramos, Florian Sulzmaier, Joanna Gawecka and Ms. Sarah Hampe for their contributions and expert technical advice. This study was supported by institutional funds from the College of Pharmacy and the University of Hawaii Cancer Center to A.S.B. and grants UVA 2005-3665 from the Dutch Cancer Society 'KWF Kankerbestrijding' and EU COST BM0805 to D.G.

References

1. Brodeur GM: Neuroblastoma: biological insights into a clinical enigma. *Nat Rev Cancer* 3: 203-216, 2003.
2. Maris JM, Hogarty MD, Bagatell R and Cohn SL: Neuroblastoma. *Lancet* 369: 2106-2120, 2007.
3. Schwenker M, Bachmann AS and Moelling K: JM4 is a four-transmembrane protein binding to the CCR5 receptor. *FEBS Lett* 579: 1751-1758, 2005.
4. Fo CS, Coleman CS, Wallick CJ, Vine AL and Bachmann AS: Genomic organization, expression profile, and characterization of the new protein PRA1 domain family, member 2 (PRAF2). *Gene* 371: 154-165, 2006.
5. Bachmann AS, Duennebieff FF and Mocz G: Genomic organization, characterization, and molecular 3D model of GDE1, a novel mammalian glycerophosphoinositol phosphodiesterase. *Gene* 371: 144-153, 2006.

6. Koomoa DL, Go RC, Wester K and Bachmann AS: Expression profile of PRAF2 in the human brain and enrichment in synaptic vesicles. *Neurosci Lett* 436: 171-176, 2008.
7. Borsics T, Lundberg E, Geerts D, *et al*: Subcellular distribution and expression of prenylated Rab acceptor 1 domain family, member 2 (PRAF2) in malignant glioma: influence on cell survival and migration. *Cancer Sci* 101: 1624-1631, 2010.
8. Sivars U, Aivazian D and Pfeffer SR: Yip3 catalyses the dissociation of endosomal Rab-GDI complexes. *Nature* 425: 856-859, 2003.
9. Compton SL and Behrend EN: PRAF1: a Golgi complex transmembrane protein that interacts with viruses. *Biochem Cell Biol* 84: 940-948, 2006.
10. Compton SL, Kemppainen RJ and Behrend EN: Prenylated Rab acceptor domain family member 1 is involved in stimulated ACTH secretion and inhibition. *Cell Signal* 21: 1901-1909, 2009.
11. Kim JT, Cho MY, Choi SC, *et al*: Prenylated Rab acceptor 1 (PRA1) inhibits TCF/beta-catenin signaling by binding to beta-catenin. *Biochem Biophys Res Commun* 349: 200-208, 2006.
12. Li LY, Shih HM, Liu MY and Chen JY: The cellular protein PRA1 modulates the anti-apoptotic activity of Epstein-Barr virus BHRF1, a homologue of Bcl-2, through direct interaction. *J Biol Chem* 276: 27354-27362, 2001.
13. Liu HP, Wu CC and Chang YS: PRA1 promotes the intracellular trafficking and NF-kappaB signaling of EBV latent membrane protein 1. *EMBO J* 25: 4120-4130, 2006.
14. Lin CI, Orlov I, Ruggiero AM, *et al*: Modulation of the neuronal glutamate transporter EAAC1 by the interacting protein GTRAP3-18. *Nature* 410: 84-88, 2001.
15. Mao WG, Liu ZL, Chen R, Li AP and Zhou JW: JWA is required for the antiproliferative and pro-apoptotic effects of all-trans retinoic acid in HeLa cells. *Clin Exp Pharmacol Physiol* 33: 816-824, 2006.
16. Chen H, Bai J, Ye J, *et al*: JWA as a functional molecule to regulate cancer cells migration via MAPK cascades and F-actin cytoskeleton. *Cell Signal* 19: 1315-1327, 2007.
17. Geerts D, Wallick CJ, Koomoa DL, *et al*: Expression of prenylated Rab acceptor 1 domain family, member 2 (PRAF2) in neuroblastoma: correlation with clinical features, cellular localization, and cerulenin-mediated apoptosis regulation. *Clin Cancer Res* 13: 6312-6319, 2007.
18. Valster A, Tran NL, Nakada M, Berens ME, Chan AY and Symons M: Cell migration and invasion assays. *Methods* 37: 208-215, 2005.
19. Fardin P, Barla A, Mosci S, *et al*: A biology-driven approach identifies the hypoxia gene signature as a predictor of the outcome of neuroblastoma patients. *Mol Cancer* 9: 185, 2010.
20. Revet I, Huizenga G, Chan A, *et al*: The MSX1 homeobox transcription factor is a downstream target of PHOX2B and activates the Delta-Notch pathway in neuroblastoma. *Exp Cell Res* 314: 707-719, 2008.
21. Barrett T, Troup DB, Wilhite SE, *et al*: NCBI GEO: archive for high-throughput functional genomic data. *Nucleic Acids Res* 37: D885-D890, 2009.
22. Bewick V, Cheek L and Ball J: Statistics review 12: survival analysis. *Crit Care* 8: 389-394, 2004.
23. Vento MT, Zazzu V, Loffreda A, *et al*: Praf2 is a novel Bcl-xL/Bcl-2 interacting protein with the ability to modulate survival of cancer cell. *PLoS One* 5: e15636, 2010.
24. Malumbres M and Barbacid M: Cell cycle, CDKs and cancer: a changing paradigm. *Nat Rev Cancer* 9: 153-166, 2009.
25. Molenaar JJ, Koster J, Ebus ME, *et al*: Copy number defects of G1-cell cycle genes in neuroblastoma are frequent and correlate with high expression of E2F target genes and a poor prognosis. *Genes Chromosomes Cancer* 51: 10-19, 2012.
26. Bai J, Zhang J, Wu J, *et al*: JWA regulates melanoma metastasis by integrin alphaVbeta3 signaling. *Oncogene* 29: 1227-1237, 2010.
27. Hynes RO: Metastatic potential: generic predisposition of the primary tumor or rare, metastatic variants - or both? *Cell* 113: 821-823, 2003.
28. Hendrix A, Westbrook W, Bracke M and De Wever O: An ex(o) citing machinery for invasive tumor growth. *Cancer Res* 70: 9533-9537, 2010.
29. Peinado H, Lavotshkin S and Lyden D: The secreted factors responsible for pre-metastatic niche formation: old sayings and new thoughts. *Semin Cancer Biol* 21: 139-146, 2011.
30. Shi GZ, Yuan Y, Jiang GJ, *et al*: PRAF3 induces apoptosis and inhibits migration and invasion in human esophageal squamous cell carcinoma. *BMC Cancer* 12: 97, 2012.